

Nonlinear asymmetric tearing mode evolution in cylindrical geometry

Cite as: Phys. Plasmas **23**, 102515 (2016); <https://doi.org/10.1063/1.4966243>

Submitted: 09 August 2016 • Accepted: 10 October 2016 • Published Online: 27 October 2016

 Q. Teng, N. Ferraro,  D. A. Gates, et al.



View Online



Export Citation



CrossMark

ARTICLES YOU MAY BE INTERESTED IN

[Saturation of the tearing mode](#)

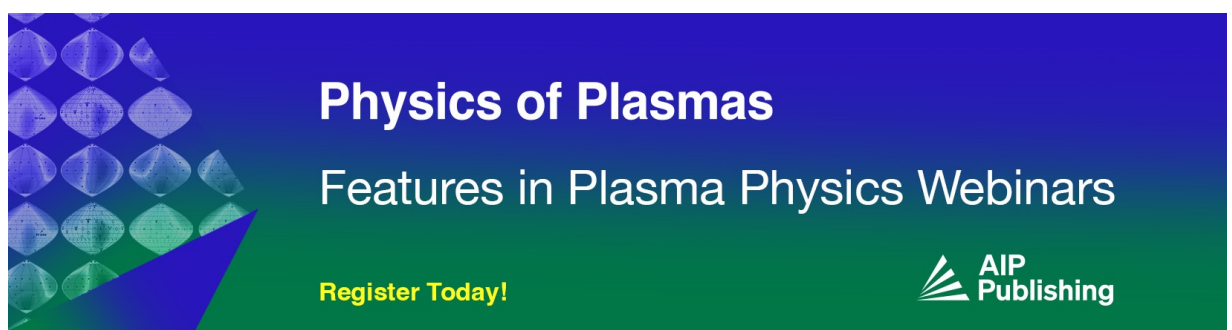
The Physics of Fluids **20**, 800 (1977); <https://doi.org/10.1063/1.861939>

[Finite-Resistivity Instabilities of a Sheet Pinch](#)

The Physics of Fluids **6**, 459 (1963); <https://doi.org/10.1063/1.1706761>

[Nonlinear growth of the tearing mode](#)

The Physics of Fluids **16**, 1903 (1973); <https://doi.org/10.1063/1.1694232>



Physics of Plasmas
Features in Plasma Physics Webinars

Register Today!



Nonlinear asymmetric tearing mode evolution in cylindrical geometry

Q. Teng, N. Ferraro, D. A. Gates, S. C. Jardin, and R. B. White

Princeton Plasma Physics Laboratory, Princeton University, P.O. Box 451, Princeton, New Jersey 08543, USA

(Received 9 August 2016; accepted 10 October 2016; published online 27 October 2016)

The growth of a tearing mode is described by reduced MHD equations. For a cylindrical equilibrium, tearing mode growth is governed by the modified Rutherford equation, i.e., the nonlinear $\Delta'(w)$. For a low beta plasma without external heating, $\Delta'(w)$ can be approximately described by two terms, $\Delta'_{ql}(w)$, $\Delta'_A(w)$ [White *et al.*, Phys. Fluids **20**, 800 (1977); Phys. Plasmas **22**, 022514 (2015)]. In this work, we present a simple method to calculate the quasilinear stability index Δ'_{ql} rigorously, for poloidal mode number $m \geq 2$. Δ'_{ql} is derived by solving the outer equation through the Frobenius method. Δ'_{ql} is composed of four terms proportional to: constant Δ'_0 , w , $w \ln w$, and w^2 . Δ'_A is proportional to the asymmetry of island that is roughly proportional to w . The sum of Δ'_{ql} and Δ'_A is consistent with the more accurate expression calculated perturbatively [Arcis *et al.*, Phys. Plasmas **13**, 052305 (2006)]. The reduced MHD equations are also solved numerically through a 3D MHD code M3D-C1 [Jardin *et al.*, Comput. Sci. Discovery **5**, 014002 (2012)]. The analytical expression of the perturbed helical flux and the saturated island width agree with the simulation results. It is also confirmed by the simulation that the Δ'_A has to be considered in calculating island saturation. *Published by AIP Publishing.* [<http://dx.doi.org/10.1063/1.4966243>]

I. INTRODUCTION

The tearing mode is a very important MHD instability in tokamaks. It may cause confinement deterioration and even disruptions as it connects the core and the edge directly. It has also long been a candidate to explain major disruptions⁵ and the tokamak density limit.^{6–9} Furth *et al.* first calculated the linear growth rate of a tearing mode in slab and cylindrical geometry.^{10,11} Rutherford then calculated the nonlinear tearing mode growth when the island width exceeds the size of the tearing layer but is still small compared with the system size.¹² White first proposed the quasilinear stability index Δ'_{ql} in Ref. 1 and added the asymmetry stability index Δ'_A in Ref. 2 to describe the island growth

$$\frac{dw}{dt} = 1.22 \frac{\eta}{\mu_0} \Delta'(w) \approx 1.22 \frac{\eta}{\mu_0} \left(\Delta'_{ql}(w) + \Delta'_A(w) \right), \quad (1)$$

where $\Delta'_{ql} = \psi_1'|_{r_l}/\psi_1(r_s)$, ψ_1 is the first harmonic of the perturbed helical flux, r_s , r_l , r_r are the minor radius of rational surface, left (inner) and right (outer) edges of the island, respectively. The helical flux ψ is defined through $\psi = 2\pi \int_0^r \vec{B} \cdot \nabla \tau r dr$, where $\tau = \theta - n\phi/m$. A more accurate constant 1.22 is used according to Ref. 13. In this work, we present a rigorous method to calculate Δ'_{ql} as an extension of the quasilinear calculation in Ref. 1. We also show that the solution of $\psi_1(r)$ in the outer region captures the island structure accurately.

II. ANALYTICAL CALCULATION OF Δ'_{ql} AND Δ'_A

This work is performed in cylindrical geometry. The variables (r, θ, z) form a right-handed coordinate system, and $\phi = z/R$ ($2\pi R$ is the periodic length in the z direction). The current density in the ϕ direction is expressed through Ampere's law

$$j = \frac{1}{\mu_0 2\pi R} \nabla_{\perp}^2 \psi_h + \frac{2n}{\mu_0 m} \frac{B_{\phi}}{R}, \quad (2)$$

where $\nabla_{\perp} = \nabla r \partial r + \nabla \theta \partial \theta$, B_{ϕ} is the $\hat{\phi}$ component of the equilibrium magnetic field. Consider a single harmonic perturbation of the helical flux

$$\psi_h(r, \tau) = \psi_0(r) + \psi_1(r) \cos(m\tau). \quad (3)$$

Outside the island, the plasma inertia is negligible. Taking the first harmonic of Eq. (2), ψ_1 is the solution of

$$\left(\frac{d^2}{dr^2} + \frac{1}{r} \frac{d}{dr} - \frac{m^2}{r^2} \right) \psi_1 = 2\pi\mu_0 R \frac{dj_0}{d\psi_0} \psi_1, \quad (4)$$

with a conducting wall boundary condition $\psi_1(a) = 0$. Expand Eq. (4) near the rational surface $r = r_s$. Let $x = r - r_s$ and keep the terms up to $O(x)$

$$\psi_1'' + (r_s^{-1} - r_s^{-2}x)\psi_1' - (Kx^{-1} + L + Mx)\psi_1 = 0, \quad (5)$$

$$K = \frac{2\pi\mu_0 R j^{(1)}}{\psi_0^{(2)}} \Big|_{r=r_s}, \quad (6)$$

$$L = \frac{m^2}{r_s^2} + \frac{2\pi\mu_0 R j^{(2)}}{\psi_0^{(2)}} - \frac{\pi\mu_0 R j^{(1)} \psi_0^{(3)}}{\left(\psi_0^{(2)}\right)^2} \Big|_{r=r_s}, \quad (7)$$

$$M = -\frac{2m^2}{r_s^3} + \pi\mu_0 R j^{(1)} \left[\frac{\left(\psi_0^{(3)}\right)^2}{2\left(\psi_0^{(2)}\right)^3} - \frac{\psi_0^{(4)}}{3\left(\psi_0^{(2)}\right)^2} \right] - \pi\mu_0 R j^{(2)} \frac{\psi_0^{(3)}}{\left(\psi_0^{(2)}\right)^2} + \pi\mu_0 R j^{(3)} \frac{1}{\psi_0^{(2)}} \Big|_{r=r_s}, \quad (8)$$

where the superscript in parentheses denotes derivative with respect to r . $x = 0$ is a regular singular point of this equation. Assume $\psi_1(x) = x^r \sum_{n=0}^{\infty} a_n x^n$, then the indicial equation is $r(r-1)a_0 = 0$. Choosing the larger solution $r_1 = 1$ gives $y_1(x) = \sum_{n=0}^{\infty} a_n x^{n+1}$, with a_0 a free parameter, and

$$a_1 = \frac{1}{2} \left(K - \frac{1}{r_s} \right) a_0, \tag{9}$$

$$a_2 = \left(\frac{1}{3r_s^2} - \frac{K}{4r_s} + \frac{1}{12}K^2 + \frac{1}{6}L \right) a_0, \tag{10}$$

$$a_n = -\frac{1}{(n+1)n} \left[\left(\frac{n}{r_s} - K \right) a_{n-1} - \left(\frac{n-1}{r_s^2} + L \right) a_{n-2} - M a_{n-3} \right], \quad n \geq 3. \tag{11}$$

Assume the second solution to be $y_2(x) = y_1(x) \cdot \ln|x| + \sum_{n=0}^{\infty} b_n x^n$. We find a recurrence relation with b_0 and b_1 two free parameters, and

$$a_0 = K b_0, \tag{12}$$

$$b_2 = -\frac{3}{2} a_1 + \frac{1}{2} \left(K - \frac{1}{r_s} \right) b_1 - \frac{1}{2r_s} a_0 + \frac{1}{2} L b_0, \tag{13}$$

$$b_n = -\frac{1}{n(n-1)} \left[(2n-1)a_{n-1} + \left(\frac{n-1}{r_s} - K \right) b_{n-1} + \frac{1}{r_s} a_{n-2} - \left(\frac{n-2}{r_s^2} + L \right) b_{n-2} - \frac{1}{r_s^2} a_{n-3} - M b_{n-3} \right], \quad n \geq 3. \tag{14}$$

There appear to be two free parameters in the second solution, but a change in b_1 only changes $y_2(x)$ by adding some multiple of $y_1(x)$. Thus, choose $b_1 = 0$, rewrite the free parameters as C_1 and C_2 , and keep terms up to $O(x^3)$, then the general solution is

$$\begin{aligned} \psi_1(x) = & C_1 \cdot \left[x + \frac{1}{2} \left(K - \frac{1}{r_s} \right) x^2 + \left(\frac{1}{3r_s^2} - \frac{K}{4r_s} + \frac{1}{12}K^2 + \frac{1}{6}L \right) x^3 \right] \\ & + C_2 \left\{ \left[x + \frac{1}{2} \left(K - \frac{1}{r_s} \right) x^2 + \left(\frac{1}{3r_s^2} - \frac{K}{4r_s} + \frac{1}{12}K^2 + \frac{1}{6}L \right) x^3 \right] \ln|x| \right. \\ & \left. + \frac{1}{K} + \left(-\frac{3}{4}K + \frac{1}{4r_s} + \frac{L}{2K} \right) x^2 + \left(-\frac{1}{9r_s^2} + \frac{5}{12} \frac{K}{r_s} - \frac{7}{36}K^2 - \frac{1}{18}L - \frac{1}{6} \frac{L}{r_s K} + \frac{1}{6} \frac{M}{K} \right) x^3 \right\}. \end{aligned} \tag{15}$$

Substituting $x = 0$, find $C_2 = K\psi_1(0)$. Rewrite C_1 as

$$C_1 = \begin{cases} -A\psi_1(0) & \text{if } x < 0, \\ -B\psi_1(0) & \text{if } x > 0, \end{cases} \tag{16}$$

then, the first order derivative of $\psi_1(x)$ for $x < 0$ is

$$\begin{aligned} \frac{\psi_1'(x)}{\psi_1(0)} = & -A \cdot \left[1 + \left(K - \frac{1}{r_s} \right) x + \left(\frac{1}{r_s^2} - \frac{3K}{4r_s} + \frac{1}{4}K^2 + \frac{1}{2}L \right) x^2 \right] \\ & + \left[1 + \left(K - \frac{1}{r_s} \right) x + \left(\frac{1}{r_s^2} - \frac{3K}{4r_s} + \frac{1}{4}K^2 + \frac{1}{2}L \right) x^2 \right] \cdot K \ln|x| \\ & + K + (-K^2 + L)x + \left(\frac{k^2}{r_s} - \frac{1}{2}K^3 - \frac{1}{2r_s}L + \frac{1}{2}M \right) x^2, \end{aligned} \tag{17}$$

and $\psi_1'(x)$ for $x > 0$ only differs by replacing A with B. For small island width w , the island is roughly symmetric. Thus, we have $x_l = r_l - r_s \approx -w/2$, $x_r = r_r - r_s \approx w/2$ and $w = 4\sqrt{\psi_1(r_s)/(-\psi_1'(r_s))}$. Then, Δ'_{ql} as a function of w is

$$\begin{aligned} \Delta'_{ql} = & A - B + \left[-(0.5A + 0.5B + 0.69K) \left(K - \frac{1}{r_s} \right) - K^2 + L \right] w \\ & + K \left(K - \frac{1}{r_s} \right) w \ln w + \frac{1}{4}(A - B) \left(\frac{1}{r_s^2} - \frac{3K}{4r_s} + \frac{1}{4}K^2 + \frac{1}{2}L \right) w^2, \end{aligned} \tag{18}$$

where the w^2 term is usually much smaller than the first three terms. The asymmetry stability index Δ'_A is due to an imbalance of the m th harmonic of the current, given by

$$\begin{aligned} \Delta'_A = & -\frac{2\pi R \mu_0 m}{\psi_1(r_s) \pi} \int_{-\pi/m}^{\pi/m} d\theta \int_{\tilde{r}_l(\theta)}^{\tilde{r}_r(\theta)} dr \delta j(r) \cos(m\theta), \tag{19} \\ \approx & -\frac{2\pi R \mu_0}{\psi_1(r_s)} f_F \frac{m}{\pi} \int_{-\pi/m}^{\pi/m} d\theta \int_{\tilde{r}_l(\theta)}^{\tilde{r}_r(\theta)} dr (j_0(r_x) - j_0(r)) \cos(m\theta), \end{aligned} \tag{20}$$

where f_F is a positive flattening factor less than 1, accounting for the degree of current profile flattening inside the island. If the left edge r_l and right edge r_r of the island are known at $\theta = 0$, the location of the island separatrix can be approximated by

$$\tilde{r}_l(\theta) = \frac{1}{2}(r_l - r_x) \cos(m\theta) + \frac{1}{2}(r_l + r_x), \tag{21}$$

$$\tilde{r}_r(\theta) = \frac{1}{2}(r_r - r_x)\cos(m\theta) + \frac{1}{2}(r_r + r_x). \quad (22)$$

Then, for the small island width

$$\Delta'_A \approx -\frac{2\pi R\mu_0}{\psi_1(r_s)}f_F \frac{m}{\pi} \int_{-\pi/m}^{\pi/m} d\theta \int_{\tilde{r}_l(\theta)}^{\tilde{r}_r(\theta)} dr (-j'_0(r_x))(r - r_x)\cos(m\theta), \quad (23)$$

$$= -\frac{2\pi R\mu_0}{\psi_1(r_s)}f_F \frac{m}{\pi} \int_{-\pi/m}^{\pi/m} d\theta \left(-\frac{1}{8}j'_0(r_x) \right) w(r_l + r_r - 2r_x) \times \cos(m\theta)(\cos(m\theta) + 1)^2, \quad (24)$$

$$= \frac{\pi R\mu_0}{2\psi_1(r_s)}f_F j'_0(r_x)w(r_l + r_r - 2r_x), \quad (25)$$

$$\approx \frac{\pi R\mu_0}{4\psi_1(r_s)}f_F (-j'_0(r_x))w^2 A_s, \quad (26)$$

$$= \frac{\mu_0 4\pi R j'_0(r_x)}{\psi''_0(r_s)} f_F A_s, \quad (27)$$

where $A_s = (r_x - r_l)/(r_r - r_x) - 1$ is a positive number representing the degree of the island asymmetry, which is roughly proportional to the island width.² This expression has been obtained in Ref. 2 though with a different numerical coefficient. In Ref. 3, Arcis *et al.* derived the nonlinear $\Delta'(w)$ using a perturbative method, giving

$$\Delta' = A - B + [-0.20(A + B)\tilde{K} - 1.81\tilde{K}^2 + 0.33\tilde{K}/r_s + 0.41\tilde{L}]w + 0.41\tilde{K}^2 w \ln w, \quad (28)$$

where $\tilde{K} = j'(r)/j(r) \cdot (1 - 2/s)|_{r_s}$, $\tilde{L} = j''(r)/j(r) \cdot (1 - 2/s)|_{r_s}$, $s = r q(r)/q(r)|_{r_s}$. In fact, simple algebra shows that $\tilde{K} = \mu_0 j^{(1)}/\psi_0^{(2)}|_{r=r_s} = K$ and $\tilde{L} = \mu_0 j^{(2)}/\psi_0^{(2)}|_{r=r_s}$. This expression has included the asymmetry effect implicitly. Eq. (28) has similar terms to the combination of Eqs. (18) and (27), except for the numerical coefficients and some higher order terms.

III. COMPARISON OF THE FROBENIUS METHOD AND NUMERICAL CALCULATION

We now compare the results of the Frobenius method with a fully nonlinear numerical calculation obtained with the code M3D-C1.⁴ The code uses a finite element representation of the radial functions and solves the reduced MHD equations in cylindrical geometry. We use the FRS equilibrium for comparison¹¹

$$j(r) = \frac{j_0}{[1 + (r/r_0)^{2\nu}]^{1+1/\nu}}, \quad q(r) = q_0 [1 + (r/r_0)^{2\nu}]^{1/\nu}, \quad (29)$$

where j_0 is the current density on the axis, r_0 is the width of the current channel, ν is a parameter controlling the peakedness of the current profile, and $q_0 = 2B_\phi/(\mu_0 R j_0)$ is the safety factor on the axis. First, Eq. (4) is solved numerically and the two constants A and B in the analytical expression

Eq. (15) are determined by fitting the semi-analytical solution of $\psi_1(x)$ with the local expansion expression near the rational surface. Then, the perturbed helical flux and its derivative are fully determined as in Eqs. (15) and (17). The case under consideration is an equilibrium with $q_0 = 1.15$, $\nu = 1.0$, $r_0 = 0.81$, unstable to the 2/1 tearing mode. In Fig. 1 are shown $\psi_1(r)$ and $\psi'_1(r)$ given by the semi-analytical calculation, Frobenius method, and simulation. The semi-analytical results agree with the fully nonlinear simulation within 1% except for some deviation of $\psi'_1(r)$ near r_s , as the simulation includes modification in the island interior. The Frobenius method results show good agreement with the semi-analytical result for $r > 0.5$. More important are the island parameters entering into any nonlinear evaluation of saturation properties. They include the island width, the positions of the outside and inside island edges, the locations of the island O-points and X-points, the island asymmetry, and the island saturation width. It is clearly seen that the shift of the O-point from the rational surface is larger than the shift of the X-point, this result is due to the difference in the mean slope of the radial eigenfunction inside and outside the rational surface, and directly related to the linear growth rate of the mode. Shown in Table I are the values given by the simulation and the local expansion. The results are seen to be

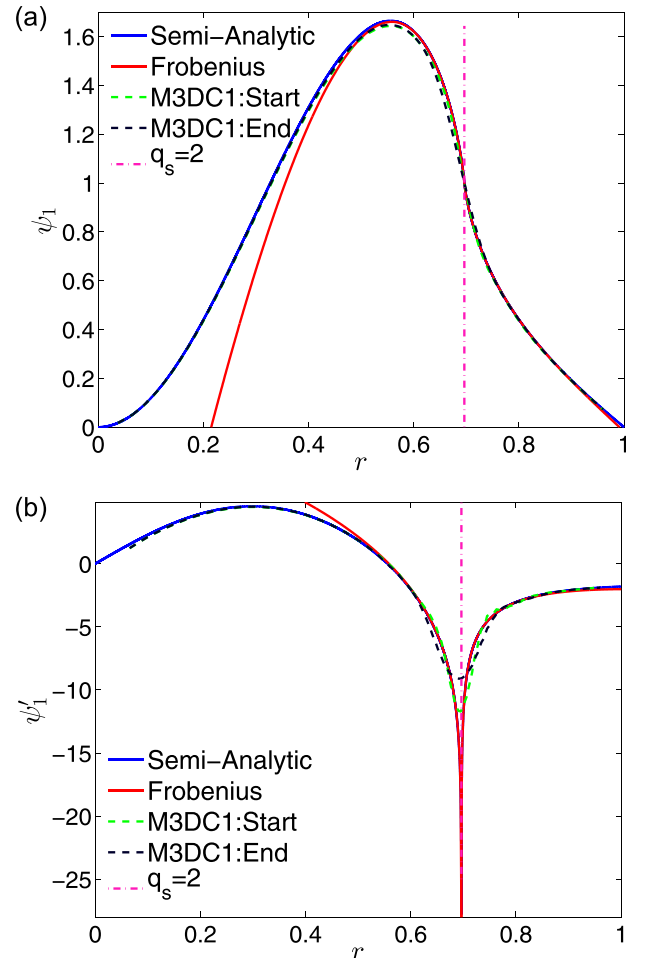


FIG. 1. Comparison of $\psi_1(r)$ and $\psi'_1(r)$. $\psi_1(r)$ is normalized to 1 at r_s . The results at the beginning of the island growth (Start) and at saturation (End) from simulation are plotted.

TABLE I. Characteristics of the magnetic island.

	r_l	r_r	r_x	r_o	r_s	A_s	w
Analytic	0.6272	0.7485	0.7051	0.6858	0.6964	0.7964	0.1214
Simulation	0.6266	0.7480	0.7036	0.6849	0.6964	0.7342	0.1214

accurate within 1% except for A_s , which is 8%. The simulation gives a saturated width of 0.1214. The semi-analytical calculation gives the same width if we use $f_F=0.17$. The degree of flattening f_F can also be calculated from the simulation result

$$f_F = \frac{\frac{m}{\pi} \int_{-\pi/m}^{\pi/m} d\theta \int_{\bar{r}_l}^{\bar{r}_r} dr (j(r, \theta) - j_0(r)) \cos(m\theta)}{\frac{m}{\pi} \int_{-\pi/m}^{\pi/m} d\theta \int_{\bar{r}_l}^{\bar{r}_r} dr (j(r_x) - j_0(r)) \cos(m\theta)}, \quad (30)$$

where $j(r, \theta)$ is the current density at saturation. This formula gives $f_F=0.25$, not very different from what the semi-analytical calculation requires.

IV. SUMMARY

In this work, Δ'_{ql} and Δ'_A are derived analytically and used to calculate island saturation. Although this method is not as accurate as Ref. 3, it is much simpler. The comparison with the numerical simulation confirms that the island asymmetry must be considered in calculating island saturation. The island characteristics, $\psi_1(r)$ and $\psi'_1(r)$, from the analytical calculation and the simulation show good agreement.

This result is important because it demonstrates that the linear eigenfunction can be used to calculate the properties of an island state, including saturation width, and that the solution external to the island is not significantly changed by the internal island dynamics.

ACKNOWLEDGMENTS

This work was supported by the U.S. Department of Energy Grant under Contract Nos. DE-AC02-09CH11466 and DE-SC0004125.

- ¹R. B. White, D. A. Monticello, M. N. Rosenbluth, and B. Waddell, *Phys. Fluids* **20**, 800 (1977).
- ²R. B. White, D. A. Gates, and D. P. Brennan, *Phys. Plasmas* **22**, 022514 (2015).
- ³N. Arcis, D. F. Escande, and M. Ottaviani, *Phys. Plasmas* **13**, 052305 (2006).
- ⁴S. C. Jardin, N. Ferraro, J. Breslau, and J. Chen, *Comput. Sci. Discovery* **5**, 014002 (2012).
- ⁵R. B. White, D. A. Monticello, and M. N. Rosenbluth, *Phys. Rev. Lett.* **39**, 1618 (1977).
- ⁶P. H. Rebut and M. Hugon, *Plasma Phys. Controlled Nucl. Fusion Res.*, London **2**, 197 (1984); see http://www.iaea.org/inis/collection/NCLCollectionStore/_Public/16/055/16055667.pdf#page=215.
- ⁷D. A. Gates and L. Delgado-Aparicio, *Phys. Rev. Lett.* **108**, 165004 (2012).
- ⁸D. A. Gates, D. P. Brennan, L. Delgado-Aparicio, and R. B. White, *Phys. Plasmas* **22**, 060701 (2015).
- ⁹Q. Teng, D. P. Brennan, L. Delgado-Aparicio, D. A. Gates, J. Swerdlow, and R. B. White, *Nucl. Fusion* **56**, 106001 (2016).
- ¹⁰H. P. Furth, J. Killeen, and M. N. Rosenbluth, *Phys. Fluids* **6**, 459 (1963).
- ¹¹H. P. Furth, P. H. Rutherford, and H. Selberg, *Phys. Fluids* **16**, 1054 (1973).
- ¹²P. H. Rutherford, *Phys. Fluids* **16**, 1903 (1973).
- ¹³R. Fitzpatrick, *Phys. Plasmas* **2**, 825 (1995).